PRAMANA — journal of physics

© Indian Academy of Sciences

Vol. 76, No. 5
May 2011
pp. 707–723

Working group report: Physics at the Large Hadron Collider

Coordinators: D K GHOSH[1,*], A NYFFELER[2] and V RAVINDRAN[2]

Working group members: N Agarwal[3], P Agarwal[4], P Bandyopadhyay[2,5], R Basu[6], B Bhattacherjee[7], S S Biswal[7], D Choudhury[8], M Dahiya[9], S Dutta[9], N Gaur[8], K Ghosh[10], R M Godbole[11], S Gopalakrishna[6,12], R Islam[8], W Kilgore[13], M Kumar[8], M C Kumar[2], S Majee[14], S Majhi[15], T Mandal[6], H S Mani[6], P Mathews[15], S Mitra[6], A Mukherjee[16], K Rao[17], V Rawoot[18], S D Rindani[19], T S Roy[20], P Saha[8], R Santos[21], S Seth[15], P Sharma[19], A Shivaji[4], R K Singh[22], J P Singh[23], R Tibrewala[6], A Tripathi[7] and M Won[24]

[1]Department of Theoretical Physics and Centre for Theoretical Sciences, Indian Association for the Cultivation of Science, Kolkata 700 032, India
[2]Harish-Chandra Research Institute, Allahabad 211 019, India
[3]Department of Physics, Allahabad University, Allahabad 211 002, India
[4]Institute of Physics, Bhubaneswar 751 005, India
[5]Korea Institute for Advanced Study, Seoul, Korea
[6]Institute of Mathematical Sciences, Chennai 600 113, India
[7]Tata Institute of Fundamental Research, Mumbai 400 005, India
[8]Department of Physics and Astrophysics, University of Delhi, Delhi 110 007, India
[9]SGTB Khalsa College, University of Delhi, Delhi 110 007, India
[10]Department of Physics, University of Calcutta, Kolkata 700 072, India
[11]Centre for High Energy Physics, Indian Institute of Science, Bangalore 560 012, India
[12]School of Physics, The University of Melbourne, Australia
[13]Physics Department, Brookhaven National Laboratory, Upton, USA
[14]CP3, Université catholique de Louvain, Louvain-la-Neuve, Belgium
[15]Saha Institute of Nuclear Physics, Kolkata 700 064, India
[16]Physics Department, Indian Institute of Technology, Mumbai 400 076, India
[17]Department of Physics, University of Helsinki, Helsinki, Finland
[18]Department of Physics, Mumbai University, Mumbai 400 032, India
[19]Physical Research Laboratory, Ahmedabad 380 009, India
[20]Department of Physics, University of Oregon, Eugene, USA
[21]NExT Institute and School of Physics and Astronomy, University of Southampton, UK
[22]Institut für Theoretische Physik und Astronomie, Universität Würzburg, Germany
[23]Department of Physics, M.S. University of Baroda, Vadodara 390 002, India
[24]LIP - Departamento de Física, Universidade de Coimbra, Coimbra, Portugal
*Corresponding author. E-mail: tpdkg@iacs.res.in

Abstract. This is a summary of the activities of the *Physics at the LHC* working group in the XIth Workshop on High Energy Physics Phenomenology (WHEPP-XI) held at the Physical Research Laboratory, Ahmedabad, India in January 2010. We discuss the activities of each sub-working

group on physics issues at colliders such as Tevatron and Large Hadron Collider (LHC). The main issues discussed involve (1) results on W mass measurement and associated QCD uncertainties, (2) an attempt to understand the asymmetry measured at Tevatron in the top quark production, and (3) phenomenology of warped space dimension model.

Keywords. Large Hadron Collider; top quark; W-mass; QCD and EW radiative corrections; extra dimensions.

PACS Nos 14.65.Ha; 14.70.Fm; 14.80.Rt; 11.10.Kk

1. Introduction

The main focus of these working group activities was to study some interesting and technically viable physics issues at two hadron colliders currently under operation, the $p\bar{p}$ collider at Tevatron (Fermilab) and pp Large Hadron Collider (LHC) at CERN.

The commencement of the LHC opens up a unique avenue to probe the particle physics at the TeV scale at an unprecedented level.

In the Standard Model (SM), electroweak gauge bosons ($W^{\pm}$, Z) and the top quark (t) represent the most massive fundamental particles so far discovered. The understanding of the electroweak symmetry breaking of the SM is highly correlated with the precise measurement of the properties of top quark and electroweak gauge bosons. Any significant deviation in the properties of the top quark, W and Z from the SM predictions may lead to a new physics scenario at the TeV scale which can be probed at both Tevatron and LHC. In this direction, precise knowledge of higher-order corrections, specially the QCD corrections to different SM processes are very important.

Several new physics models have been proposed to solve the gauge hierarchy problem of the SM which can be tested at the LHC. All these new models produce a plethora of new particles which may lead to interesting collider signatures both at Tevatron and LHC.

Keeping all these in mind and the available skills and interests of the members of this working group, some problems were identified and discussed. In this short report, we summarize such problems and the follow-up work.

2. W Boson mass working group report

N Agarwal, S Biswal, D K Ghosh, R Godbole, W B Kilgore, M C Kumar, S Majhi, P Mathews, S Mitra, A Mukherjee, A Nyffeler, V Ravindran, S Seth, P Sharma, A Shivaji, J P Singh and A Tripathi

2.1 *Introduction*

The W boson mass working group discussed the current status of the W boson mass measurement and the prospects for improving LEP and Tevatron measurements at the LHC. The

W boson mass is a very important parameter in the Standard Model. In the absence of radiative corrections, it is related to the mass of the Z boson by the relative coupling strengths of the $SU(2)_L$ and $U(1)_Y$ gauge interactions that mix under spontaneous symmetry breaking to form the photon and the massive weak bosons,

$$\frac{M_W}{M_Z} = \frac{g}{\sqrt{g^2 + g'^2}}. \tag{1}$$

Of course, radiative corrections break this simple relation, but lead to a more complicated relation involving the masses of the Standard Model particles as well as the masses of any beyond-the-standard-model particles that carry electroweak charge. The most important radiative corrections within the Standard Model involve the top quark, which are enhanced because of its large mass splitting with the b quark.

The Higgs boson mass is the most important unknown parameter involved, although the radiative corrections are only logarithmically dependent on its value. Nonetheless, measurements of the masses of the top quark and W boson constrain the mass of a Standard Model Higgs boson as shown in figure 1.

At hadron colliders, the W boson mass is determined by making precise measurements of the observables of the leptonic (e or μ) decay modes, p_{T}^{ℓ}, p_{T}^{ν}, m_{T}^{W}, the transverse momentum of the charged lepton, the transverse momentum of the unobserved neutrino, and the transverse mass of the W boson respectively. The transverse momentum of the charged lepton is measured through a combination of tracking and calorimetry,

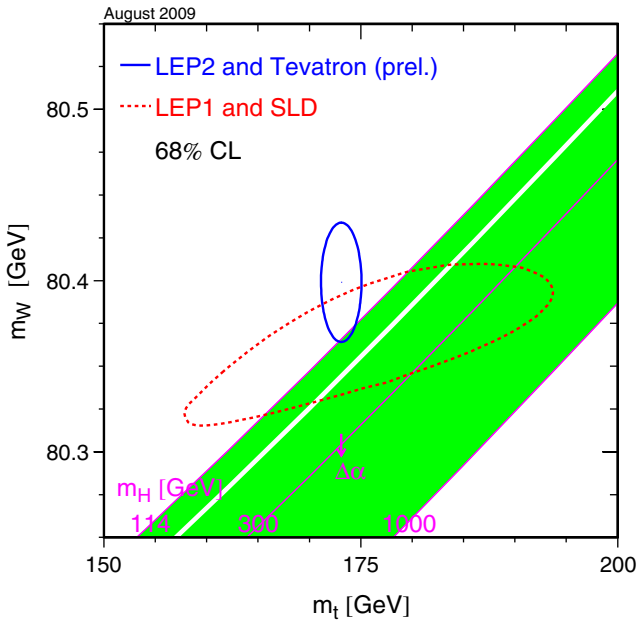

Figure 1. Mass constraint on a Standard Model Higgs boson from M_W and M_t.

the transverse momentum of the neutrino is inferred from the missing transverse momentum needed to balance the event and the transverse mass is computed as $M_{\mathrm{T}}^{W} = \sqrt{2p_{\mathrm{T}}^{\ell}p_{\mathrm{T}}^{\nu}(1-\cos\phi_{\ell\nu})}$.

The charged lepton spectrum is of course the best measured distribution, but it is subject to significant radiative corrections. The transverse mass is theoretically more stable, but relies upon the inferred values of p_{T}^{ν} and $\phi_{\ell\nu}$. The standard technique for determining the W boson mass at the Tevatron experiments is to measure the desired distributions for the Z boson, fit these measurements to the best available theoretical calculation, and then form templates at narrowly spaced mass intervals, of the expected shapes of the W boson distributions. The best-fitting template determines the W boson mass [1,2].

The rates for W and Z production are known to next-to-next-to-leading order in QCD [3,4], but the shapes of distributions are strongly affected by resummation effects. The Tevatron experiments therefore use the resummed next-to-leading order QCD calculation RESBOS [5,6] to fit the Z boson distributions. In particular, they fit for nonperturbative shape functions that parametrize the Z boson transverse momentum distribution and then use those same shape coefficients to predict the W boson transverse momentum distribution and the resulting change in shape of the lepton distributions.

This procedure works quite well at the Tevatron and has led to the most precise measurements of the W boson mass, but is a procedure optimized for relatively low Z boson statistics. Fitting for the nonperturbative parameters makes efficient use of the Z sample, at the price of increasing the systematic uncertainty through the choice of more or less arbitrary fitting parameters.

At the LHC, the Z boson production rate will be quite large and it should be possible to leverage the high statistics measurement of the Zs to improve the W boson measurements. One suggestion for doing this is to use the 'ratio method' [7]. The idea is to compute the lepton distributions for W and Z bosons, appropriately scaled by the masses, and use the ratio of the calculated distributions to scale the measured Z boson distributions into a prediction of the W boson distributions

$$\left(\frac{\mathrm{d}\sigma^{W}}{\mathrm{d}p_{\mathrm{T}}^{\ell}}\right)_{\text{predicted}} = \left(\frac{\mathrm{d}\sigma^{W}/\mathrm{d}p_{\mathrm{T}}^{\ell}}{\mathrm{d}\sigma^{Z}/\mathrm{d}p_{\mathrm{T}}^{\ell}}\right)_{\text{theory}} \left(\frac{\mathrm{d}\sigma^{Z}}{\mathrm{d}p_{\mathrm{T}}^{\ell}}\right)_{\text{measured}}. \tag{2}$$

One of the advantages of this method is that one does not need resummed calculations to form the ratios. This fact stems from the universality of the leading infrared structure of gauge theories that allow one to even perform resummation. The general form of a cross-section computed to nth order in perturbation theory is

$$\frac{\mathrm{d}\sigma_{V}^{(n)}}{\mathrm{d}p_{\mathrm{T}}} = \frac{\mathrm{d}\sigma_{V}^{(0)}}{\mathrm{d}p_{\mathrm{T}}} \sum_{l=1}^{n}\sum_{m=0}^{2l-1} a_{l,m}^{V}\alpha_{s}^{l}\log^{m}(p_{\mathrm{T}}/\mu) + R_{n}(\alpha_{s}), \tag{3}$$

where $\sigma_{V}^{(0)}$ is the tree-level cross-section. As $p_{\mathrm{T}} \to 0$, the logarithms become large and the leading logarithmic terms dominate. These are precisely the terms that get resummed. The

universality of the leading infrared structure means that $a^V_{l,2l-1}$ is the same for any vector boson V, which in turn means that

$$\lim_{p_T \to 0} \frac{d\sigma^{(n)}_W/dp_T}{d\sigma^{(n)}_Z/dp_T} = \frac{d\sigma^{(0)}_W/dp_T}{d\sigma^{(0)}_Z/dp_T}. \tag{4}$$

Even as $p_T \to 0$ and resummation effects become most pronounced, the ratio method, using unresummed calculations, becomes exact! This means that the ratio method can take advantage of any fixed-order calculations, NLO QCD, NLO electroweak, etc., as they become available.

The measurements at the Tevatron are already dominated by systematic uncertainties. The prospects for improving the precision of the W mass measurement at the LHC will depend upon reducing these systematic uncertainties [8,9]. To achieve a precision of 20 MeV or less, it will also be necessary to reduce the theoretical uncertainty of the analysis. Therefore, as the LHC begins operations, we feel that it is time to take a new look at the ratio method and to study how the inclusion of increasingly precise calculations will decrease the theoretical uncertainty in the determination of the W boson mass.

2.2 *Questions*

The questions that the working group hopes to address are:

- How well do we want to know the W boson mass? At what point does increased precision cease to constrain new physics?
- What is the current theoretical uncertainty on the W boson mass, and how far can it be reduced? Using the ratio method, what level of precision is obtained as one includes increasingly precise theoretical input such as NLO QCD, NLO electroweak, NNLO QCD, etc.?

Beyond the immediate scope of the W boson mass measurement, the ratio method might prove useful for benchmarking expected signals for new physics. Therefore, we also consider the question

- Can we extend the ratio method to normalize gluon-induced cross-sections such as $pp \to t\bar{t}$ or $pp \to H$ from quark-gluon initiated processes like $pp \to Z$+jet?

References

[1] T Aaltonen *et al* (CDF), *Phys. Rev.* **D77**, 112001 (2008), 0708.3642
[2] V M Abazov *et al* (D0), *Phys. Rev. Lett.* **103**, 141801 (2009), 0908.0766
[3] R Hamberg, W L van Neerven and T Matsuura, *Nucl. Phys.* **B359**, 343 (1991)
[4] R V Harlander and W B Kilgore, *Phys. Rev. Lett.* **88**, 201801 (2002), hep-ph/0201206
[5] C Balazs and C P Yuan, *Phys. Rev.* **D56**, 5558 (1997), hep-ph/9704258
[6] F Landry, R Brock, P M Nadolsky and C P Yuan, *Phys. Rev.* **D67**, 073016 (2003), hep-ph/0212159
[7] W T Giele and S Keller, *Phys. Rev.* **D57**, 4433 (1998), hep-ph/9704419

[8] V Buge *et al*, *J. Phys.* **G34**, N193 (2007)
[9] N Besson, M Boonekamp, E Klinkby, T Petersen and S Mehlhase (ATLAS), *Eur. Phys. J.* **C57**, 627 (2008), 0805.2093

3. New physics contributions to $A_{\rm FB}^t$ at Tevatron

S S Biswal, D Choudhury, M Dahiya, S Datta, R M Godbole, R Islam, M Kumar, M C Kumar, S Majhi, H S Mani, P Mathews, S Mitra, K Rao, V Ravindran, V Rawoot, S D Rindani, P Saha, R Santos, P Sharma, R K Singh and M Won

Abstract. We discuss the possible new physics approaches to explain the large $A_{\rm FB}^t$ observed at Tevatron. The approaches and partial results are presented.

3.1 *Introduction*

The top quark is produced in $p\bar{p}$ collisions at Tevatron via strong interactions mechanism. For unpolarized beams of protons and anti-protons, the angular distribution of top-quark is expected to be symmetric at the leading order owing to the parity and charge conjugation invariance of QCD. However, at the higher order in the perturbation theory, one expects a nonzero forward–backward asymmetry for top quark, $A_{\rm FB}^t = 0.05 \pm 0.015$ [1], originated from the interference of C-even and C-odd amplitudes. On the other hand, the asymmetry measured at Tevatron is found to be large, $A_{\rm FB}^t = 0.19 \pm 0.065\,(\text{stat}) \pm 0.024\,(\text{syst})$ [2] in the laboratory frame with 3.2 fb^{-1} of data [2a]. The deviation from the SM prediction is about 2σ ($\sim 1.5\sigma$ with new data) and there is some scope for explaining this via new physics. In this note we sketch several ways to fill the gap between the experimental observation and the theoretical prediction.

The idea is to find a new cause that leads to a sizable asymmetry $A_{\rm FB}^t$ without changing the total cross-section $\sigma_{t\bar{t}}^{\rm tot}$ or differential cross-section $\mathrm{d}\sigma_{t\bar{t}}/m_{t\bar{t}}$ beyond the experimental errors. Additionally, one can also look at the top polarization and polarization correlation as an additional observable that may help us to distinguish between different new physics possibilities.

3.2 *New physics interactions at tree level*

One way to fill the gap between the SM prediction and experimental values is by introducing new particles mediating the production process. For completeness, we consider scalar, vector or tensor particles exchanged in s- or t-channel. The new particle should contribute to $u\bar{u}/d\bar{d} \to t\bar{t}$ as these are the relevant channels at Tevatron. We note that any s-channel exchange requires the couplings of the new particles to be chiral in order to create a tree-level $A_{\rm FB}^t$. On the other hand, t-channel exchange does not require chiral couplings but they are flavour changing (usually neutral) currents.

- For a new vector in s-channel, we require it to be a colour octet to interfere with the SM amplitude and provide sizable asymmetry. This can be easily found in models with warped extra dimensions and has been studied in ref. [4]. An axigluon (a new

model) is also studied in ref. [5]. A vector in t-channel, on the other hand, can be either colour singlet [6] or octet and can have either parity conserving or violating couplings and still give a large asymmetry owing to the t-channel kinematics. A detailed study of all these possibilities are under progress [7].

- We do not have any additional contribution to the asymmetry from a scalar in the s-channel exchange, owing to the spherical distribution in scalar to fermion pair decay. However, a flavour changing interaction in t/u-channel exchange can contribute to the asymmetry. A t-channel exchange of colour triplet and sextet has been studied in ref. [8] and a u-channel diquark exchange in ref. [9]. A generic colour singlet and octet possibility is also under consideration [7].
- Another possibility is the parity violating or the flavour violating tensor particle exchange in s-channel or t-channel, respectively. This possibility with different kinds of couplings are under consideration [7].

In all the above cases we would like to study the correlation between the top polarization and $A_{\rm FB}^t$. This analysis was carried out in [10] and the results are summarized in §3.3.

3.3 *Top polarization and forward–backward asymmetry in $t\bar{t}$ production*

The large forward–backward asymmetry ($A_{\rm FB}$) in $t\bar{t}$ production reported at the Tevatron continues to elicit much interest [4–6,8,9,11]. The latest experimental report [3] quotes $A_{\rm FB} \sim 15\%$ whereas within the SM one expects $A_{\rm FB} \sim 5\%$ [1]. As discussed in §3.2, many possible new physics (NP) scenarios have been offered as explanations for this observation.

Naively, a nonzero $A_{\rm FB}$ seems to be an indication of some violation of a discrete symmetry and, indeed, most models that purport to explain this anomaly have invoked a parity-violating interaction for the top quark. Even though this assumption certainly holds true for any s-channel NP contribution to $q\bar{q} \to t\bar{t}$, clearly, it is not applicable when t- or u-channel contributions are present as well. In other words, the measured $A_{\rm FB}$, in the presence of any NP interactions, may accrue from either explicit parity violation (dynamics) or the effects of t-(u-) channel propagators (kinematics) or a combination of both.

Forward–backward asymmetry, at the Tevatron, is defined as

$$A_{\rm FB} = \frac{\sigma(\cos\theta_t > 0) - \sigma(\cos\theta_t < 0)}{\sigma(\cos\theta_t > 0) + \sigma(\cos\theta_t < 0)}, \tag{5}$$

where θ_t is the angle made by the top quark with the direction of the proton in the lab-frame.

Analogously, a single top polarization asymmetry ($A_{\rm P}$) can be defined as

$$A_{\rm P} = \frac{\sigma(+) - \sigma(-)}{\sigma(+) + \sigma(-)}\,, \tag{6}$$

where $+$ or $-$ denotes the helicity of the top quark, and the helicities of $\bar{t}$ are summed over. The SM prediction for this arises due to electroweak effects and is expected to be small.

This observable has the advantage of catching the essence of the parity violating effect characteristic of the differently suggested new physics models and thus, it may be expected,

would be able to distinguish between different competing NP scenarios. In addition, it provides an advantage in terms of the statistics that may be obtained as it requires the knowledge of the polarization of only the top. Other similar observables, such as spin correlation coefficients etc., involve measurement of the polarization of the top as well as the anti-top, and hence, are experimentally more challenging.

Of new physics models that have been studied in this context, we choose for comparison, the triplet diquark model [8], the flavour violating Z' model [6] and the flavour nonuniversal axigluon model [5]. A detailed discussion of these models and the emergence of $A_{\rm FB}$ and $A_{\rm P}$ in them can be found in ref. [10].

We scan the parameter space for each of these models with the restriction that the couplings be perturbative. Further, taking hints from various phenomenological and experimental studies [6,12,13], we adopt the mass limits $M_\Phi > 350$ GeV, $M_{Z'} > 120$ GeV and $M_A < 1400$ GeV.

The parameter spaces thus defined, the numerical calculation is done using a parton level Monte Carlo routine. We use the CTEQ6L [14] parton distributions with the factorization scale set to m_t with the latter held to 172.5 GeV to be consistent with the value used in measurements of cross-section [15] and $A_{\rm FB}$ [3]. A K-factor [16] of 1.3 is used to estimate the cross-section at NLO [16a].

For each parameter-space point we calculate the cross-section, $A_{\rm FB}$ and $A_{\rm P}$, as defined above. In figure 2, we show the correlation between $A_{\rm P}$ and $A_{\rm FB}$ for each of the three models along with the experimentally allowed $1-\sigma$ band for $A_{\rm FB}$. One feature immediately stands out. For the regions that are consistent with the measured $A_{\rm FB}$ values, there is no overlap between the three models.

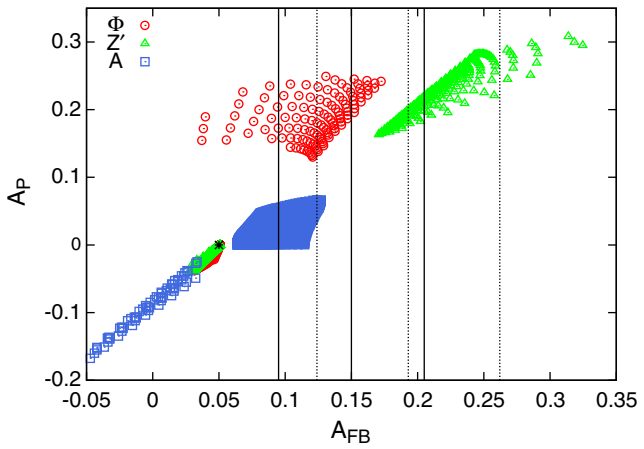

Figure 2. Correlation between $A_{\rm P}$ and $A_{\rm FB}$ for different models. All the points shown are consistent with the experimentally observed cross-section at the $1-\sigma$ level and with restrictions on $M_{\rm boson}$ as described in the text. The vertical solid (dotted) lines correspond to the central value and $1-\sigma$ bands of the new (old) CDF measurement of $A_{\rm FB}$, namely $15.0\% \pm 5.5\%$ ($19.3\% \pm 6.9\%$). The 'star' corresponds to the SM value at NLO.

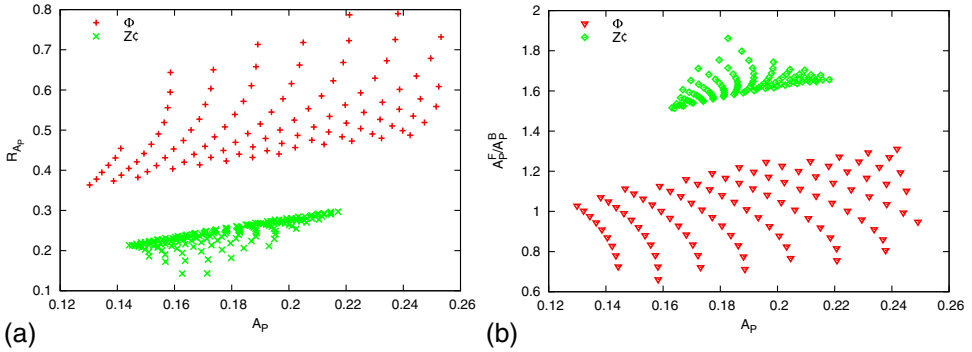

Figure 3. (**a**) R_{A_P} vs. A_P; (**b**) correlation between the ratio of A_P in the forward and backward hemispheres and total A_P. All the points depicted are consistent with the measurement of $\sigma(t\bar{t})$ and A_{FB} at the $1-\sigma$ level.

While this picture looks promising, one can see that there still exist regions of parameter space where both diquarks and Z's produce similar values of A_P (∼16–20%). With a view to make a further distinction between the two models, we evaluate the ratios R_{A_P} and $R_{A_{FB}}$ where

$$R_A = \frac{A(|\Delta y| < 1)}{A(|\Delta y| \geq 1)} \tag{7}$$

and Δy is the difference between the rapidities of the top and the anti-top. We find that, the diquark and Z' models populate different regions in the R_{A_P}–A_P and $R_{A_{FB}}$–A_{FB} planes. The separation is particularly distinct in the R_{A_P}–A_P plane (figure 3a), where diquarks can be seen to produce always a value of R_{A_P} greater than ~ 0.33, while for Z', R_{A_P} always is less than this value.

R_{A_P}, however, is not the only direction-dependent asymmetry variable. Of the many such possible variables, we consider only one, namely, A_P as calculated separately for the forward and backward hemispheres. In particular, we plot, in figure 3b, the ratio of A_P in the two hemispheres against the total A_P. Again, one finds that the diquark and Z' models give rise to markedly different correlations.

We conclude that, with experimental errors under control, a combination of observables as described above, can be expected to distinguish between the 'explanations' for the A_{FB} 'anomaly' quite successfully.

3.4 *Effective operators approach*

Instead of adding new particles to the Lagrangian, one can also add new operators with the SM particles content that respect the $SU(3)_c \times SU(2)_L \times U(1)_Y$ symmetry. In other words, the new physics scale is high enough to be integrated out and it only appears through the higher dimension operators. A complete set of such observables can be found in ref. [17]. We, however, restrict ourself only to those operators that can contribute to $p\bar{p} \to t\bar{t}$. These operators can be divided into two categories:

1. Four-fermion operators.

$$\mathscr{L}_6^{4F} = \frac{g_s^2}{\Lambda^2}\sum_{A,B}\big[C_{1q}^{AB}(\bar{q}_A\gamma_\mu q_A)(\bar{t}_B\gamma^\mu t_B) + C_{8q}^{AB}(\bar{q}_A T^a\gamma_\mu q_A)(\bar{t}_B T^a\gamma^\mu t_B)\big], \tag{8}$$

where $T^a = \lambda^a/2$, $\{A, B\} = \{L, R\}$, $q = (u, d)^T/(s, c)^T$ and the suffix $1q(8q)$ denotes colour singlet (octet) interaction. There are eight such operators for every quark flavour q. Since we have dominant contribution to $t\bar{t}$ production through $u\bar{u}$ fusion, we restrict to $q = u$, i.e. only eight operators.

2. Fermion–boson operators: $\mathscr{L}_6 = \frac{1}{\Lambda^2}\sum_i \mathcal{O}_i$, where $\mathcal{O}_i$s are

$$\begin{aligned}
&\mathcal{O}_{uG} = i\alpha_1\,\bar{u}\lambda^a\gamma^\mu\gamma_R D^\nu t G^a_{\mu\nu} && \mathcal{O}_{uG} = i\alpha_2\,\bar{t}\lambda^a\gamma^\mu\gamma_R D^\nu u G^a_{\mu\nu}\\
&\mathcal{O}_{uG'} = \alpha_3\,\bar{q}^u\lambda^a\sigma^{\mu\nu}\gamma_R t\tilde{\varphi}G^a_{\mu\nu} && \mathcal{O}_{uG'} = \alpha_4\,\bar{q}^t\lambda^a\sigma^{\mu\nu}\gamma_R u\tilde{\varphi}G^a_{\mu\nu}\\
&\mathcal{O}_{uB} = i\alpha_5\,\bar{u}\gamma^\mu\gamma_R D_\nu t B^{\mu\nu} && \mathcal{O}_{uB} = i\alpha_6\,\bar{t}\gamma^\mu\gamma_R D_\nu u B^{\mu\nu}\\
&\mathcal{O}_{uW} = \alpha_7\,\bar{q}^u\tau^I\sigma^{\mu\nu}\gamma_R t\tilde{\varphi}W^{I,\mu\nu} && \mathcal{O}_{uW} = \alpha_8\,\bar{q}^t\tau^I\sigma^{\mu\nu}\gamma_R u\tilde{\varphi}W^{I,\mu\nu}\\
&\mathcal{O}_{uB'} = \alpha_9\,\bar{q}^u\sigma^{\mu\nu}\gamma_R t\tilde{\varphi}B_{\mu\nu} && \mathcal{O}_{uB'} = \alpha_{10}\,\bar{q}^t\sigma^{\mu\nu}\gamma_R u\tilde{\varphi}B_{\mu\nu}\\
&\mathcal{O}_{Du} = \alpha_{11}\,\bar{q}^u\gamma_R(D^\mu t)(D_\mu\tilde{\varphi}) && \mathcal{O}_{\bar{D}u} = \alpha_{12}\,(D^\mu\bar{q}^u)\gamma_R t(D_\mu\tilde{\varphi})\\
&\mathcal{O}_{\varphi u} = i\alpha_{13}\,\varphi^\dagger(D_\mu\varphi)\bar{u}\gamma^\mu\gamma_R t && \mathcal{O}_{\varphi u} = i\alpha_{14}\,\varphi^\dagger(D_\mu\varphi)\bar{t}\gamma^\mu\gamma_R u\\
&\mathcal{O}_{uG} = i\alpha_{15}\,\bar{c}\lambda^a\gamma^\mu\gamma_R D^\nu t G^a_{\mu\nu} && \mathcal{O}_{uG} = i\alpha_{16}\,\bar{t}\lambda^a\gamma^\mu\gamma_R D^\nu c G^a_{\mu\nu}\\
&\mathcal{O}_{uG'} = \alpha_{17}\,\bar{q}^c\lambda^a\sigma^{\mu\nu}\gamma_R t\tilde{\varphi}G^a_{\mu\nu} && \mathcal{O}_{uG'} = \alpha_{18}\,\bar{q}^t\lambda^a\sigma^{\mu\nu}\gamma_R c\tilde{\varphi}G^a_{\mu\nu}
\end{aligned} \tag{9}$$

where τ^I are the Pauli matrices ($I = 1, 2, 3$), $\gamma_{R,L} = (1 \pm \gamma_5)/2$ and α_i are the coefficients of the operators. The list above contains operators that are not constrained by the flavour constraints.

The first kind of operator can be either flavour changing or flavour conserving depending on the underlying physics that give rise to them. On the other hand, the second kind of operators are flavour changing and unconstrained by the flavour physics. We study these two sets of operators separately.

3.4.1 *Four-fermion operators.* In the analysis with four-fermion operators, we have a total of eight different kinds of operators, four with $t\bar{t}$ in colour octet state and the other four in colour singlet state. We note that the colour singlet operators do not interfere with the dominant SM diagrams $u\bar{u} \to g \to t\bar{t}$, and hence can create the asymmetry only through the modulus square terms and interference with γ/Z mediated diagrams. This usually gives

Table 1. The best fit value of the coefficients of the four-fermion operators. The $m_{t\bar{t}}$ distribution of this fit point is shown in figure 4. The asymmetry for this best fit point is $A_{\rm FB}^t = 0.143$.

C_{8q}^{LL}	C_{8q}^{RR}	C_{8q}^{LR}	C_{8q}^{RL}	C_{1q}^{LL}	C_{1q}^{RR}	C_{1q}^{LR}	C_{1q}^{RL}
+0.97	+0.48	−0.89	−0.97	+0.06	−0.07	−0.03	−0.01

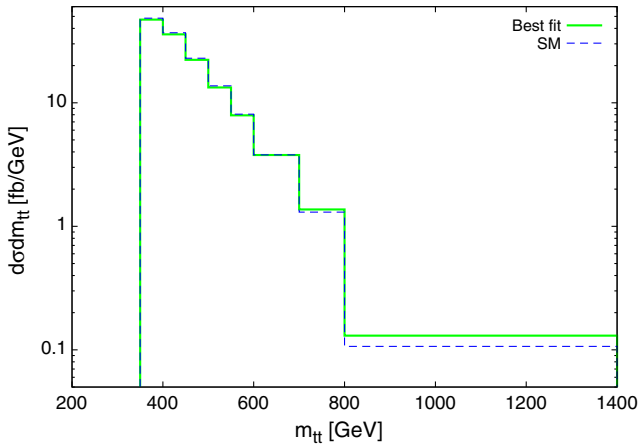

Figure 4. The differential cross-section for the SM and SM with four-fermion operators for the best fit point (see table 1), which leads to $A^t_{\rm FB} = 0.143$.

very small asymmetry. One needs to have large couplings for the electroweak operators to get sizable asymmetry but that leads to a sizable contribution to both the cross-section and the differential distribution. Colour octet operators, on the other hand, yield large asymmetry for small enough changes in the cross-sections. Further, the contribution to asymmetry and cross-sections are different for different operators and they can combine to give a large asymmetry and small contribution to the cross-section. To this end, we perform a global fit of these eight operators to $A^t_{\rm FB}$, $\sigma^{\rm tot}_{t\bar{t}}$ and $\mathrm{d}\sigma_{t\bar{t}}/m_{t\bar{t}}$ via Markov-Chain-Monte-Carlo (MCMC) method and found that only the colour octet operators are favoured with $\mathcal{O}(1)$ coefficients while color singlet operators are disfavoured with $\mathcal{O}(10^{-2})$ coefficients (see table 1). The $m_{t\bar{t}}$ distribution of this fit point is shown in figure 4. The details of this study will be presented elsewhere [18].

3.4.2 *Fermion–boson operators.* The analysis with fermion–boson operators involves 18 operators listed in eq. (9). It is possible to have some more operators contributing to the top pair production process, but those are constrained by flavour physics and hence simply dropped from our analysis. The total cross-section and asymmetry have been calculated for all these operators considered one at a time and the χ^2 of the fit has been studied. It has been found that some of the operators lead to negative values of the asymmetries for any couplings and large contributions to the cross-sections, when considered one at a time. However, it is not clear *a priori* if the interference of these operators with others will be useful or not. Thus, a complete analysis with selected set of useful operators and all three observables using the MCMC method is performed using $A^t_{\rm FB}$, $\sigma^{\rm tot}_{t\bar{t}}$ and $\mathrm{d}\sigma_{t\bar{t}}/m_{t\bar{t}}$ as observables. We found the asymmetry to be $A^t_{\rm FB} = 0.107$ for the best fit point with $\chi^2_{\rm min} = 6$. The detailed analysis of these findings will be presented elsewhere [18].

3.5 *Loops in extra-dim models*

We know that the leading order contribution to $A^t_{\rm FB}$ in the SM comes from the box diagram, i.e. $\mathcal{O}(\alpha_s^3)$ terms in the cross-section. Thus, the obvious extension of the 'tree level new

physics' approach is to stick to some model, say extra-dimension model, which has KK-gluon and perform a full one-loop calculation of the asymmetry in this chosen model. This model, in general, can lead to a tree-level contribution to the asymmetry and also at one loop via the box diagrams. We note that chiral coupling of new particles is not required to generate additional contributions to the asymmetry at loop level. If the KK-gluon has chiral couplings to the fermions, as in Randall–Sundrum model, then more diagrams, like vertex correction etc., can also add to (or subtract from) the asymmetry. Some partial, but dominant, contributions have recently been calculated in ref. [19]. The complete calculations in this direction are under progress [20].

3.6 *Summary*

In this report, we have summarized some of the possible approaches to incorporate new physics contribution to the forward–backward asymmetry (or the charge asymmetry) of the top quark observed at Tevatron. Some of the approaches have been pursued since their proposal in WHEPP and a glimpse of some results are shown.

References

[1] O Antunano, J H Kuhn and G Rodrigo, *Phys. Rev.* **D77**, 014003 (2008)
J H Kuhn and G Rodrigo, *Phys. Rev. Lett.* **81**, 49 (1998)

[2] The CDF Collaboration: *Measurement of the forward–backward asymmetry in $t\bar{t}$ production in 3.2 fb^{-1} of $p\bar{p}$ collisions at $\sqrt{s} = 1.96$* TeV, March 2009, CDF/ANAL/TOP/PUBLIC/9724; http://www-cdf.fnal.gov/physics/new/top/2009/tprop/Afb/

[2a] A recent analysis with 5.3 fb^{-1} of data shows $A_{\rm FB}^t = 0.15 \pm 0.050\,(\text{stat}) \pm 0.024\,(\text{syst})$ [3] in the laboratory frame

[3] The CDF Collaboration: *Measurement of the inclusive forward–backward asymmetry and its rapidity dependence $A_{fb}(|\Delta y|)$ of $t\bar{t}$ production in 5.3 fb^{-1} of Tevatron data*, CDF/ANAL/TOP/PUBLIC/10224, http://www-cdf.fnal.gov/physics/new/top/2010/tprop/Afb/

[4] A Djouadi, G Moreau, F Richard and R K Singh, arXiv:0906.0604 [hep-ph]

[5] P H Frampton, J Shu and K Wang, *Phys. Lett.* **B683**, 294 (2010), arXiv:0911.2955 [hep-ph]

[6] S Jung, H Murayama, A Pierce and J D Wells, *Phys. Rev.* **D81**, 015004 (2010), arXiv:0907.4112 [hep-ph]

[7] S Datta *et al*, in preparation

[8] J Shu, T M P Tait and K Wang, *Phys. Rev.* **D81**, 034012 (2010), arXiv:0911.3237 [hep-ph]

[9] A Arhrib, R Benbrik and C H Chen, arXiv:0911.4875 [hep-ph]

[10] D Choudhury, R M Godbole, S D Rindani and P Saha, arXiv:1012.4750 [hep-ph]

[11] C H Chen *et al*, arXiv:1009.4165 [hep-ph]
Y k Wang *et al*, arXiv:1008.2685 [hep-ph]
B Xiao *et al*, *Phys. Rev.* **D82**, 034026 (2010), arXiv:1006.2510 [hep-ph]
Q H Cao *et al*, *Phys. Rev.* **D81**, 114004 (2010), arXiv:1003.3461 [hep-ph]
V Barger *et al*, *Phys. Rev.* **D81**, 113009 (2010), arXiv:1002.1048 [hep-ph]
J Cao *et al*, *Phys. Rev.* **D81**, 014016 (2010), arXiv:0912.1447 [hep-ph]
K Cheung *et al*, *Phys. Lett.* **B682**, 287 (2009), arXiv:0908.2589 [hep-ph]
C Degrande *et al*, arXiv:1010.6304 [hep-ph]
M V Martynov *et al*, arXiv:1010.5649 [hep-ph]
I Dorsner *et al*, *Phys. Rev.* **D81**, 055009 (2010), arXiv:0912.0972 [hep-ph]

G Burdman *et al*, arXiv:1011.6380 [hep-ph]
E Alvarez *et al*, arXiv:1011.6557 [hep-ph]
R S Chivukula *et al*, *Phys. Rev.* **D82**, 094009 (2010), arXiv:1007.0260 [hep-ph]
D W Jung *et al*, *Phys. Lett.* **B691**, 238 (2010), arXiv:0912.1105 [hep-ph]
J Cao *et al*, arXiv:1011.5564 [hep-ph]
D W Jung *et al*, arXiv:1011.5976 [hep-ph]
[12] D Choudhury, M Datta and M Maity, *Phys. Rev.* **D73**, 055013 (2006)
[13] CDF Collaboration: T Aaltonen *et al*, *Phys. Rev. Lett.* **102**, 222003 (2009)
[14] J Pumplin *et al*, *J. High Energy Phys.* **0207**, 012 (2002), arXiv:hep-ph/0201195
[15] CDF Conference Note 9913, http://www-cdf.fnal.gov/physics/new/top/public_xsection.html
[16] M Cacciari *et al*, *J. High Energy Phys.* **0809**, 127 (2008), arXiv:0804.2800 [hep-ph]
[16a] In the absence of NLO calculations that incorporate the new physics effects under consideration, we use the SM K-factor
[17] W Buchmuller and D Wyler, *Nucl. Phys.* **B268**, 621 (1986)
[18] S S Biswal *et al*, in preparation
[19] M Bauer, F Goertz, U Haisch, T Pfoh and S Westhoff, arXiv:1008.0742 [hep-ph]
[20] S Majhi *et al*, in preparation

4. Phenomenology of warped-space custodian b'

S Gopalakrishna, T Mandal, S Mitra and R Tibrewala

Abstract. Warped-space models with custodial protection of the T-parameter and the $Zb\bar{b}$ coupling have extra fermions, the custodians, which can be significantly lighter than the other Kaluza–Klein excitations. We discuss the phenomenology of a custodian b' and compute its decay width and branching ratio into tW, bZ and Zh decay channels.

4.1 *Theoretical framework*

A warped-space extra dimension has been proposed [1] as a solution to the gauge hierarchy problem of the Standard Model (SM). By letting SM fields propagate in the bulk, the fermion mass hierarchy of the SM can also be addressed without badly violating FCNC constraints. Furthermore, due to the AdS/CFT duality conjecture [2], these constructions may be dual to close-to-conformal four-dimensional strongly coupled theories.

Precision electroweak constraints place strong bounds on such constructions. Gauging $SU(2)_R$ in the bulk offers a custodial symmetry that protects [3] the T-parameter. We therefore take the gauge group to be $SU(2)_L \times SU(2)_R \times U(1)_X$ under which the third-generation quarks transform as

$$Q_L \equiv (\mathbf{2}, \mathbf{1})_{1/6} = (t_L, b_L), \quad Q_{b_R} \equiv (\mathbf{1}, \mathbf{2})_{1/6} = (t'_R, b_R),$$

$$Q_{t_R} \equiv (\mathbf{1}, \mathbf{2})_{1/6} = (t_R, b'_R)\ .$$

The extra fields t'_R and b'_R (the 'custodians') are ensured to be without zero modes by applying Dirichlet–Neumann $(-, +)$ boundary conditions (BC) on the extra-dimensional

interval $[0, \pi R]$, whereas the SM particles are the zero modes of fields with Neumann–Neumann $(+,+)$ BC. The $(-,+)$ fields are most likely the lowest mass KK excitation [3, 4], and among them the b'_R couplings to SM states are bigger owing to a larger mixing with SM states, since the mixing is proportional to the larger top Yukawa coupling. Therefore, the b'_R promises to have the best observability and we shall focus on its phenomenology [4a]. So far the L, R denoted the gauge group, but from here on, for notational ease, we shall denote b'_R simply as b', and by $b'_{L,R}$ we shall mean the two Lorentz chiralities of the vector-like b'.

The theory has been analysed in greater detail in ref. [7]. The dominant mass mixing terms as given there are

$$\mathscr{L} \supset -\left(\overline{b}_L \;\; \overline{b'}_L\right) \begin{pmatrix} \lambda_{Q_L b_R} v/\sqrt{2} & \lambda_{Q_L b'_R} v/\sqrt{2} \\ 0 & M_{b'} \end{pmatrix} \begin{pmatrix} b_R \\ b'_R \end{pmatrix} + \text{h.c.}, \tag{10}$$

where the effective 4D Yukawa couplings are given by

$$\lambda_{Q_L b_R} = \frac{\tilde{\lambda}_b}{2k\pi R} f_{Q_L}(\pi R) f_{b_R}(\pi R), \tag{11}$$

which is the b-quark Yukawa coupling, and

$$\lambda_{Q_L t_R} = \frac{\tilde{\lambda}_t}{2k\pi R} f_{Q_L}(\pi R) f_{t_R}(\pi R) \tag{12}$$

is the top-quark Yukawa coupling, where $\tilde{\lambda}_{b,t}$ are the (dimensionless) 5D Yukawa couplings and f_ψ are the fermion wave functions which depend on the fermion bulk mass parameters c_ψ [8]. We have $m_b \approx \lambda_{Q_L b_R} v/\sqrt{2}$ and $m_t \approx \lambda_{Q_L t_R} v/\sqrt{2}$ to leading order ignoring the mixing to the heavier fermion KK modes, and we define the off-diagonal mass $\tilde{m} \equiv \lambda_{Q_L b'_R} v/\sqrt{2}$ for notational ease. A representative choice that is phenomenologically acceptable is: $c_{Q_L} = -0.5$; $c_{Q_{t_R}} = -0.5$; $c_{Q_{b_R}} = 0.56$, for which we have $\lambda_{Q_L b_R} = 0.025$, $\lambda_{Q_L t_R} = 1$ and $\lambda_{Q_L b'_R} = 1$.

The above mass matrix is diagonalized by biorthogonal rotations, and we denote the sine (cosine) of the mixing angles by $s_\theta^{L,R}$ ($c_\theta^{L,R}$). We denote the corresponding mass eigenstates as $(b_1\, b_2)$. The mixing angles are

$$\tan(2\theta_L) = -\frac{2\tilde{x}}{(1-\tilde{x}^2-x_b^2)}\,; \quad \tan(2\theta_R) = -\frac{2x_b\tilde{x}}{(1+\tilde{x}^2-x_b^2)}\,, \tag{13}$$

where $x_b \equiv m_b/M_{b'}$ and $\tilde{x} \equiv \tilde{m}/M_{b'}$. The mass eigenvalues to leading order in x_b are: $m_b/\sqrt{1+\tilde{x}^2}$ and $M_{b'}\sqrt{(1+\tilde{x}^2)(1+x_b^2\tilde{x}^2/(1+\tilde{x}^2)^2)}$.

We ignore $t \leftrightarrow t'$ mixing as the off-diagonal mixing term in this case is proportional to $\lambda_{Q_L b_R}$, which is small. For simplicity we also ignore the mixing in the gauge boson sector i.e., $V_\mu^{(0)} \leftrightarrow V_\mu^{(1)}$ where $V_\mu = \{W_\mu, Z_\mu\}$, since this mixing is of order $(v/M_{KK})^2$, and the gauge boson KK mass is constrained to be $\gtrsim$2 TeV by precision electroweak constraints [8a].

By going from the (b, b'_R) basis to the mass basis (b_1, b_2), the following interaction terms of b_2 were found:

$$\begin{aligned}\mathscr{L}_{4D} \supset & -\frac{e}{3}\bar{b}_2\gamma^\mu b_2 A_\mu + g_s\bar{b}_2\gamma^\mu T^\alpha b_2 g_\mu^\alpha - \left(\frac{g s_\theta^L}{\sqrt{2}}\bar{t}_{1L}\gamma^\mu b_{2L} W_\mu^+ + \text{h.c.}\right) \\ & + g_Z\left(-\frac{1}{2}s_\theta^{L\,2} + \frac{1}{3}s_W^2\right)\bar{b}_{2L}\gamma^\mu b_{2L} Z_\mu \\ & + \left[g_Z c_\theta^L s_\theta^L\left(\frac{1}{2}\right)\bar{b}_{1L}\gamma^\mu b_{2L} Z_\mu + \text{h.c.}\right] \\ & + g_Z\left(\frac{1}{3}s_W^2\right)\bar{b}_{2R}\gamma^\mu b_{2R} Z_\mu, \end{aligned} \tag{14}$$

where $g_Z \equiv \sqrt{g^2 + g'^2}$, A_μ is the photon and g_μ the gluon. The Higgs interactions are given by

$$\begin{aligned}\mathscr{L}_{4D} \supset -\frac{h}{\sqrt{2}} \Big[& \bar{b}_{1L} b_{1R}\big(c_\theta^L c_\theta^R \lambda_{Q_L b_R} + c_\theta^L s_\theta^R \lambda_{Q_L b'_R}\big) + \bar{b}_{2L} b_{2R}\big(s_\theta^L s_\theta^R \lambda_{Q_L b_R} \\ & - s_\theta^L c_\theta^R \lambda_{Q_L b'_R}\big) + \bar{b}_{1L} b_{2R}\big(-c_\theta^L s_\theta^R \lambda_{Q_L b_R} + c_\theta^L c_\theta^R \lambda_{Q_L b'_R}\big) \\ & + \bar{b}_{2L} b_{1R}\big(-s_\theta^L c_\theta^R \lambda_{Q_L b_R} - s_\theta^L s_\theta^R \lambda_{Q_L b'_R}\big)\Big] + \text{h.c.} \end{aligned} \tag{15}$$

The model we are considering here has no custodial protection for the Zbb coupling and therefore shifts. If we take this model the way it is, requiring that this shift be less than about 1% roughly implies that $s_\theta^L < 0.1$ is required, i.e. $M_{b'} \gtrsim 10\,\tilde{m}$ is required. But as we have mentioned, since we have in mind application to the model in ref. [5] where this coupling is protected by the custodial symmetry, we shall consider quite light $M_{b'}$ when we discuss the phenomenology.

4.2 *Phenomenology*

The heavy mass eigenstate b_2, once produced, decays via the off-diagonal interaction terms in eqs (14) and (15). The main decay modes are $b_2 \to tW,\ b_1 Z, b_1 h$. The decay widths are given by

$$\begin{aligned}\Gamma(b_2 \to q V_\mu) = & \frac{\kappa_{b_2 tV}^2}{32\pi} M_{b_2}\left(\frac{1}{x_V^2} + 1 - 2x_{tV}^2 + x_t^2 - 2x_V^2 + x_{tV}^2 x_t^2\right) \\ & \times(1 + x_V^4 + x_b^4 - 2x_V^2 - 2x_b^2 - 2x_V^2 x_b^2)^{1/2}\,, \end{aligned} \tag{16}$$

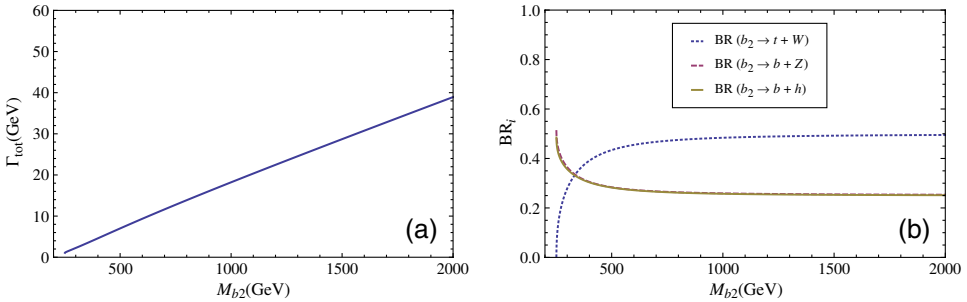

Figure 5. Total width (**a**) and BR (**b**) of b_2 versus M_{b_2}. In figure 5b, the bZ and bh decay channel curves are almost on top of each other.

$$\Gamma(b_2 \to b_1 h) = \frac{1}{16\pi} M_{b_2} \Big(\kappa^{a\,2}_{b_2 bh} \Big(1 - x_h^2 + \frac{x_b}{2} + x_b^2 \Big) + \kappa^{b\,2}_{b_2 bh} (1 - x_h^2 - 2x_b + x_b^2) \Big) \times (1 + x_h^4 + x_b^4 - 2x_h^2 - 2x_b^2 - 2x_h^2 x_b^2)^{1/2} \,, \tag{17}$$

where $V_\mu = \{W_\mu, Z_\mu\}$, $q = \{t, b\}$, $x_i = m_i/M_{b_2}$, $x_{ij} = m_i/m_j$, $\kappa_{b_2 tW} = g s_\theta^L/\sqrt{2}$, $\kappa_{b_2 bZ} = g_z s_\theta^L c_\theta^L/2$, $\kappa^a_{b_2 bh} = \left[(c_\theta^L s_\theta^R + s_\theta^L c_\theta^R) \lambda_{Q_L b_R} + (s_\theta^L s_\theta^R - c_\theta^L c_\theta^R) \lambda_{Q_L b'_R} \right] / 2\sqrt{2}$ and $\kappa^b_{b_2 bh} = \left[(c_\theta^L s_\theta^R - s_\theta^L c_\theta^R) \lambda_{Q_L b_R} - (s_\theta^L s_\theta^R + c_\theta^L c_\theta^R) \lambda_{Q_L b'_R} \right] / 2\sqrt{2}$.

Although the $b_2 bh$ coupling is large (given by $\lambda_{Q_L b'_R} = 1$), the Γ_{qV} dependence on $1/x_V^2$ enhances this partial width for large M_{b_2}, making it comparable to Γ_{bh}. This term is due to the contribution of the longitudinal polarization of V_μ. Figure 5a shows the total decay width and figure 5b shows the branching ratios (BR) as a function of M_{b_2}. The total width is about 2% of the mass in the entire range. Its roughly linear dependence on M_{b_2} can be understood by noting that (in the large M_{b_2} limit) $s_\theta^L \propto 1/M_{b_2}$, $c_\theta^L \approx 1$, leaving a $\Gamma_i \sim M_{b_2}$ behaviour for all the partial widths. All three modes have comparable branching ratios. For the tW channel, for M_{b_2} not too much bigger than m_t, the phase space suppression due to the large top mass is significant, but is overcome for large M_{b_2}. Curiously, the bZ and bh BR curves lie on top of each other. This can be understood as follows: neglecting the (small) x_b, the $b_2 b_1 Z$ and $b_2 b_1 h$ couplings are proportional to $g_Z c_\theta^L s_\theta^L$ and $c_\theta^L \lambda_{Q_L b'_R}$ respectively. Since $s_\theta^L \propto \lambda_{Q_L b'_R}$ and in the bZ partial width the factor of g_Z^2 cancels against the $1/m_Z^2$, the two BRs end up being equal as can be shown using eqs (16) and (17).

4.3 *LHC signatures*

For reasons already mentioned, b_2 can be significantly lighter than all the other KK particles, making its observability at the LHC promising. Pair production via $q\bar{q}/gg \to b_2 \bar{b_2}$ can lead to a sizeable cross-section [7]. Each b_2 decays as above and can lead to promising discovery channels. Single production of b_2 is also possible [7] via the off-diagonal couplings in eqs (14) and (15), which can be important for large M_{b_2}. These are the subject of our ongoing investigations.

Acknowledgement

We thank the organizers of WHEPP-XI at the Physical Research Laboratory, Ahmedabad for a very productive workshop.

References

[1] L Randall and R Sundrum, *Phys. Rev. Lett.* **83**, 3370 (1999), hep-ph/9905221
[2] J M Maldacena, *Adv. Theor. Math. Phys.* **2**, 231 (1998), *Int. J. Theor. Phys.* **38**, 1113 (1999), hep-th/9711200
[3] K Agashe, A Delgado, M J May and R Sundrum, *J. High Energy Phys.* **0308**, 050 (2003), hep-ph/0308036
[4] K w Choi and I W Kim, *Phys. Rev.* **D67**, 045005 (2003), hep-th/0208071
[4a] Although we show for simplicity the quark representations above, we have also in mind application to the model [5], where the $Z\bar{b}_L b_L$ coupling is protected by custodial symmetry in which the quark doublet is enlarged to $Q_L \equiv (\mathbf{2}, \mathbf{2})_{2/3}$ and e.g. $Q_{t_R} \equiv (\mathbf{1}, \mathbf{3})_{2/3} \oplus (\mathbf{3}, \mathbf{1})_{2/3}$. The effects we present here will have analogues in such models also and is the subject of ref. [6]
[5] K Agashe, R Contino, L Da Rold and A Pomarol, *Phys. Lett.* **B641**, 62 (2006), hep-ph/0605341
[6] S Gopalakrishna, G Moreau, R K Singh, in preparation
[7] S Gopalakrishna, G Moreau, R K Singh, Contribution 11, p. 129, In: G Brooijmans *et al*, 1005.1229 [hep-ph]
[8] T Gherghetta and A Pomarol, *Nucl. Phys.* **B586**, 141 (2000), hep-ph/0003129
[8a] $V_\mu^{(0)} \leftrightarrow V_\mu^{(1)}$ mixing has an additional enhancement of $k\pi R$ for an IR brane localized Higgs due to which this mixing can be important [9]
[9] C Dennis, M Karagoz Unel, G Servant and J Tseng, hep-ph/0701158